AN ABSTRACT OF THE THESIS OF

JOHN CAMERON McCULLOCH (Name) for the M. S. (Degree)

in CHEMISTRY (Major) presented on [illegible] (Date)

Title: THE ELECTRICAL PROPERTIES OF VANADIUM PENTOXIDE

Abstract approved: Redacted for Privacy

Allen B. Scott

The dc conductivity of single crystals of vanadium pentoxide was measured in the three crystallographic directions. The temperature range examined was -165°C to +25°C. The activation energy of the conduction process was isotropic and found to be .56 ev. The conductivity was anisotropic.

Measurements of the Hall effect were attempted with a dc and ac apparatus, but the signal was too low to be observed. However, an upper limit of 71 $cm^3$/coulomb for the Hall coefficient was calculated, and the upper limit computed for the mobility was .4 $cm^2$/volt sec.

A model is proposed for the conduction mechanism. It suggests that the electrical conduction is a two-step process. The electron is ionized from a $V^{4+}$-oxygen-vacancy center and then moves through the lattice via polaron movement. This model accounts for the isotropy of the activation energy and also the anisotropy of the conductivity. In addition, the dielectric constant is calculated to be 25 assuming the proposed model.

# The Electrical Properties of Vanadium Pentoxide

by

John Cameron McCulloch

A THESIS

submitted to

Oregon State University

in partial fulfillment of
the requirements for the
degree of

Master of Science

June 1968

APPROVED:

Redacted for Privacy

Professor of Chemistry

Redacted for Privacy

Head of Department of Chemistry

Redacted for Privacy

Dean of Graduate School

Date thesis is presented

Typed by Muriel Davis for John Cameron McCulloch

## ACKNOWLEDGMENTS

The ideas, thoughts and techniques described in this thesis are the product of many years of work and experience, much of which was not spent by the author. I am deeply indebted to Dr. Allen B. Scott for his guidance, instruction and criticism in not only the preparation of this thesis, but also in assisting this fledgling scientist down the road toward professionalism.

The author was fortunate to have illuminating discussions with Sir Nevill Mott regarding the polaron theory. In addition, I am grateful to Dr. W. J. Fredericks for his valuable suggestions regarding the Hall measurement apparatus.

I wish to express my thanks to Professor J. C. Looney for his generosity in allowing me to use the facilities in the Electrical Engineering Department.

I would like to acknowledge the assistance of Charles Bryden who lay much of the foundation for the present work and also made the studies with the polarizing microscope.

The author is appreciative of the financial support received from the Office of Naval Research without which this work could not have been conducted.

Lastly, but certainly not least, I wish to thank my wife Annetta for her encouragement, patience and understanding.

TABLE OF CONTENTS

LIST OF FIGURES

# THE ELECTRICAL PROPERTIES OF VANADIUM PENTOXIDE

## INTRODUCTION

In the past decade much interest has been shown in the electrical properties of the 3d transition metal oxides. The large range in valence character suggests a great variety of energy band structures and transport processes. The constituents of the series display vast differences in their electrical properties. For example, $V_2O_3$ is a metallic conductor at room temperature whereas NiO is an insulator with a conductivity 12 orders of magnitude smaller. $TiO_2$ is known to have ferroelectric properties. However, among these differences are many similarities. They all exhibit semiconduction in some temperature region, but the carriers have a low mobility. Impurities affect the conduction much less than in the covalent semiconductors (e.g., Si, Ge). Most are antiferromagnetic and change their conduction behavior at the Néel temperature. Such a group demonstrating so many differences and similarities stimulates the imagination to probe for new and more comprehensive models to explain these results.

Several attempts have been made to treat the series with one model. Morin suggested that conduction occurs via overlap of the 3d antibonding orbitals (19). However at higher atomic numbers the nuclear attraction predominates over electron-electron repulsion,

and the orbitals do not overlap for oxides with a cation heavier than vanadium. In the heavier cation oxides, he indicates that conduction occurs through local levels or exceedingly narrow bands. Heikes and Johnston studied four heavier oxides (MnO, CoO, NiO, CuO) and concluded that conduction was by a polaron mechanism (13) (see discussion). This involves the electron trapping itself by polarizing the surrounding lattice. The movement is thermally activated. By considering the mechanism to be a diffusion process, they were able to explain the change in conduction behavior at the Néel temperature.

Most of the studies on these oxides have been carried out on sintered samples. Single crystal data is very sparse. Many of the conclusions deduced from transport properties on sintered specimens have been misleading due to grain boundary effects.

The oxides of vanadium are a sub-group of the series and reveal almost all of the electrical properties of the transition metal oxides. The vanadium oxides have been studied in the vicinity of their Néel temperatures and can be classified in the following three categories (15).

1. Phases exhibiting a transition from semiconductor to metal with a discontinuous change in conductivity of the order of $10^5$ - $10^6$ $ohm^{-1}cm^{-1}$. ($V_2O_3$, $VO_2$, VO)
2. Phases having a transition from semiconduction to

semiconduction with an abrupt change in conductivity of the order of 10 - $10^2$ $ohm^{-1}cm^{-1}$. ($V_4O_7$, $V_6O_{13}$). The activation energy in the low temperature region was less than that in the high temperature region.

3. Phases exhibiting no significant change. ($V_7O_{13}$, $V_2O_5$, $V_5O_9$)

Vanadium pentoxide is used primarily as a catalyst for oxidation-reduction reactions. This property has led many investigators to study its electrical properties in order to determine a relationship between the catalytic and electrical properties of $V_2O_5$. However, it has never been determined whether the observed conductivity is intrinsic or extrinsic; hence, any exact relationship is still unclear. Evidence will be given later for extrinsic conduction.

There are eleven oxides of vanadium which have been observed at room temperature (2), and in $V_2O_5$ the vanadium exists in its highest oxidation state. It is known that $V_6O_{13}$ can exist in equilibrium with $V_2O_5$ at room temperature (2). Hence, nonstoichiometry can easily occur. Since the degree of nonstoichiometry is only a rough estimation (see page 6) the variation of the defect concentration in crystalline material with the equilibrium oxygen partial pressure at crystal growth is not known. However, since the vanadium is in its highest oxidation state in $V_2O_5$, nonstoichiometric defects should produce only n-type conduction. In addition, $V_2O_5$ is

diamagnetic; consequently, it should not exhibit any sudden change in conductivity at a Néel temperature as other oxides do.

It was mentioned above that many investigations of the electrical conductivity have been made; however most of the reported data conflict in the low temperature region. A detailed examination will be given later, but for now a short summary will suffice. Haemers indicates that two conduction processes are occurring, a high temperature process predominating above 140°K and a low temperature process predominating below 140°K (12). Boros found that the Arrhenius equation was applicable down to 120°K with a constant activation energy (5). Patrina and Ioffe observed a continuous change in activation energy to lower values at lower temperatures (21).

## Objective of the Present Work

The primary purpose of the present work was to resolve some of the controversy in the previous conductivity measurements outlined above and give a possible reason for the disagreement in the data observed. In addition, no author has studied the conductivity in all three crystallographic directions of single crystals in the low temperature region. Therefore a comprehensive study would be more revealing.

Although details of the mechanism of electronic conduction are

not known, it is generally assumed that it involves charge transfer between ions of different valence. Measurements of the Hall effect at various temperatures provide a useful tool in determining the conduction mechanism. Hall measurements not only reveal the sign of the predominant carrier but also indicate the mobility and its behavior with respect to temperature when used in conjunction with conductivity data. Therefore Hall measurements, in addition to conductivity measurements, were made in an attempt to give a greater insight into the conduction mechanism in $V_2O_5$.

In addition, research is currently being conducted in this laboratory on the electrochemical properties of single-crystalline $V_2O_5$. A knowledge of the electrical conductivity would be useful in determining the electric potential gradient in the electrode.

# EXPERIMENTAL

## Crystal Growth

The crystals were grown from Fisher Reagent grade compound. Fisher Company claims an assay content of 100.0% $V_2O_5$; their analysis also reveals .01% chlorine and .003% iron present. In addition, magnetic susceptibility measurements in another laboratory indicate nonstoichiometry and indicate that the composition of the Fisher Reagent grade powder is $V_2O_{4.9}$ (1).

The compound was poured into a platinum crucible which was cemented in an Alundum crucible placed in a Hevi Duty type 86 furnace. The temperature was monitored with a chromel-alumel thermocouple and regulated by a Leeds and Northrup Micromax controller and recorder. The system was designed such that when a relay was in the "off" position some current was still heating the furnace due to a resistance in parallel with the relay. This provided a more stable temperature in the furnace than a simple "on-off" arrangement.

The $V_2O_5$ powder was heated until melted. When the system had reached equilibrium at the melting point temperature, a seed crystal was dropped into the melt. The seed normally used was a microtome shaving from a previously grown crystal. If such a seed

were unavailable, the melt could have been supercooled until a crystallite formed. With the seed present on the surface of the melt, it was necessary to raise the temperature slowly and carefully until only a single crystallite remained. Once a very small single seed was obtained, the melt was cooled at a rate of about $1^{o}C$ every four minutes. After the melt had cooled 15 to $20^{o}C$, the crystal was lifted out of the melt with a spatula. The spatula was dipped into the melt, and the sample froze onto it. It was important to determine when the seed was single and should be allowed to grow. A small penlight was used to examine the crystal.

A single crystal has the appearance of a platelet with a dark mirror-like surface on one side. It has a layer-like structure with each plane parallel to the mirror surface, which is the $\vec{a}\vec{c}$ crystallographic plane. Dimensions of the crystals were commonly 15 x 10 x 2 mm.

An effort was made to keep the system at or below the melting point in order to avoid dissociation of the $V_2O_5$. Most of the crystals used were pulled from the melt within four hours after melting. This was done to minimize the amount of dissolved platinum. Allersma, et al. (1), report finding .02% platinum in their crystals. However they held their melt at $800^{o}C$ for three hours before growing crystals in order to "ensure constancy of composition." In the work described above, the temperature was rarely over $700^{o}C$.

In order to determine whether or not the crystals grown were single, a polarizing microscope was used. $V_2O_5$ is known to crystallize in the orthorhombic system (16). Orthohombic crystals give rise to extinction once in every $90^{\circ}$ through which the crystal is rotated on the stage of the polarizing microscope with the polarizer and analyzer crossed (8, p. 254-255). This indicates that at every $90^{\circ}$ the optic axis of the crystal is parallel to either the polarizer or the analyzer. Optic axes are defined as directions parallel to which there is no double refraction. The single crystallinity of the sample was established by moving a thinly sliced crystal into various positions without changing its orientation relative to the polarizer. As different parts of the crystal were thus observed, it was noted in each case that the angles of extinction were $0^{\circ}$ and $90^{\circ}$ consistently. If the sample were polycrystalline, different areas would yield different extinction angles.

A point of interest was the way in which $V_2O_5$ crystals grow. They grow significantly faster in the $\vec{c}$-axis direction (14). In addition, the ratio of the length to width of the crystals appeared to be proportional to the rate of cooling; i. e., the faster they were cooled, the greater was the ratio of the $\vec{c}$-axis direction to that of the $\vec{a}$-axis direction.

Crystal growing is often referred to as an art rather than a science, and the statement is especially true of this method.

Patience, trial and error, and luck are required to develop the technique.

This method was a modified version of one referred to very briefly in a paper by Boros (5). We are indebted to him for supplying us with further details through private communication.

## Preparation of Samples

The first step in preparing the crystals was slicing them with an American Optical Company microtome Model 860. This served several purposes. Polycrystalline material on the back side, which was formed upon withdrawing the crystal from the melt, was removed. The sample was shaved to a uniform thickness. In addition, some of the shavings were used as seeds for crystal growth. In order that the shaved side of the sample might be parallel to the mirror side, the pedestal was aligned on the microtome before the crystal was placed on it. The sample was then mounted on the pedestal with the $\hat{a}\hat{c}$ plane against the flat surface using Apiezon W wax to secure it in position. The sample was sliced ten microns on each cut until it had a thickness in the range of .25 - .5 mm. Trichloroethylene was used to dissolve the Apiezon W wax after the slicing.

In the next step gold was evaporated onto the crystals to provide low resistance contacts. It was found that thorough cleaning with petroleum ether and ethanol was mandatory for strongly

adhering gold leaf. The evaporation was done in a Mikros VE-10 vacuum evaporator. This apparatus consisted of a bell jar which was readily evacuated with a fore-pump and oil diffusion pump, in addition to a current source used to heat a filament for gold evaporation. The apparatus was modified slightly to provide additional current leads into the bell jar, a high-voltage electrode, and a needle-valve-controlled argon gas line into the chamber.

The bell jar was pumped to a pressure of .5 microns, and then the needle valve was opened until an equilibrium pressure of 10 microns was realized. Voltage was then applied to the high voltage electrode by a variable transformer with its output stepped up by a 20: 1 rectifying ac transformer. A blue-violet corona discharge resulted at about 400 volts and 10 microns pressure. The crystal was made the cathode. Consequently, the positive argon ions resulting from the discharge were attracted to the crystal and other cathodic parts in the bell jar. This method of "ion bombardment" was an additional step in cleaning the crystal. The ions colliding against the crystal serve to release gases adsorbed onto the surface. The bombardment was continued for at least fifteen minutes, and then the pressure was reduced to .5 microns.

After bombardment the crystal was heated with a small ceramic heater with nichrome wire serving as the heating filament. The crystal was heated to about 300$^{o}$C for fifteen minutes.

With the crystal at 300°C gold was evaporated onto the desired areas of the crystal. Those areas were determined by the size and shape of the mask used to cover the sample. For evaporation gold was placed in a small aluminum oxide crucible molded around a tungsten wire heating filament. The evaporation process was repeated on the other side of the crystal on areas opposite to those of the first deposition.

A diagram of some of the masks used may aid the reader in visualizing what was done.

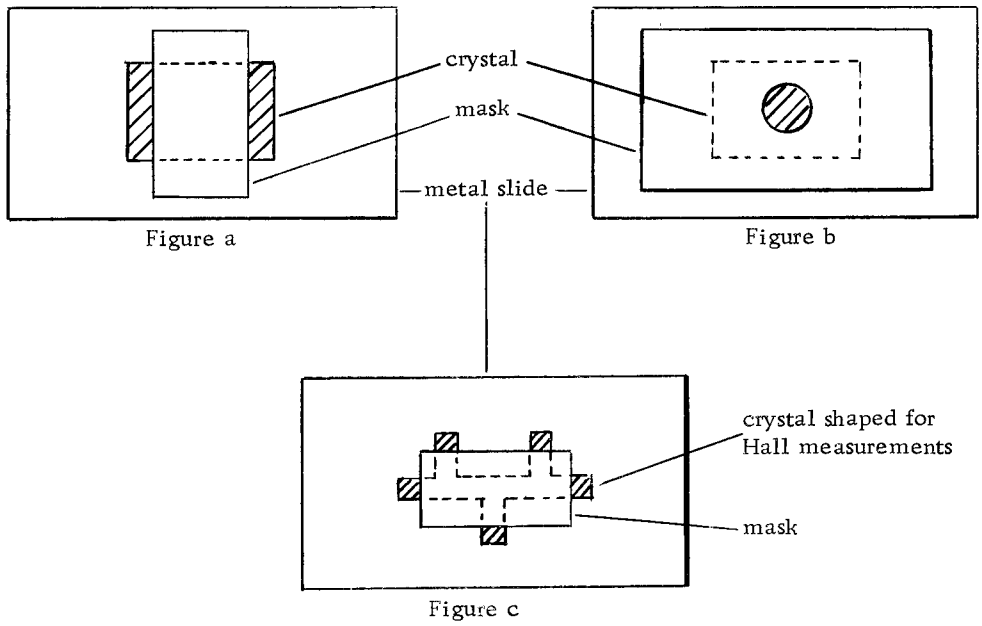


Figure a

Figure b

Figure c

Figure a represents a configuration for conductivity measurements in the $\vec{a}$ or $\vec{c}$ directions of the crystal. Figure b is the configuration for conductivity measurements in the $\vec{b}$-axis direction through

the crystal. Figure c is an illustration of the mask used for evaporation of gold onto Hall samples. The crosshatched area indicates where gold was deposited.

Some measurements were made in the $\vec{b}$- axis direction with a guard ring configuration. This necessitated an additional evaporation with a circular mask slightly larger than the hole in the mask used in the first evaporation. The net result appears as follows:

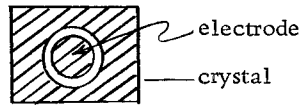


The slide and masks were made of steel. Both the masks and the slide were sanded and then lapped very smooth with 600 mesh silicon carbide in order that they would fit flatly against the crystal and not allow any evaporated gold to be deposited between the mask and the crystal. The masks were held in place by either Hoffman clamps or else phosphor bronze springs. The phosphor bronze springs were welded to the metal slide and shaped to hold the mask in place.

Although measures had been taken to keep gold from depositing in unwanted areas on the crystal, it was observed that a very small amount condensed on the side of the crystal. The amount was so small, in fact, that it did not manifest itself until conductivities of $10^{-7}$ $ohm^{-1}cm^{-1}$ at $-120^{o}C$ were measured. An illustration may

be helpful.

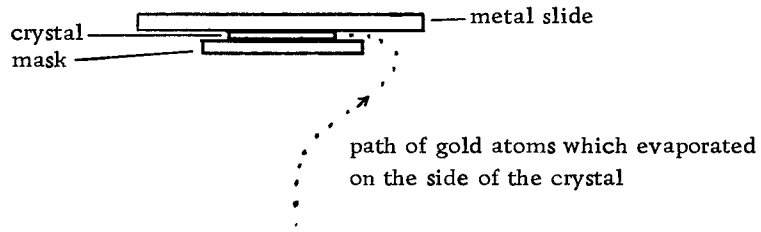


Consequently, after gold evaporation it was necessary to remove this layer of gold by scraping with a razor blade. An alternative method was to trim the sides where unwanted gold atoms might have deposited. An S. S. White Airbrasive unit Model F was used for the cutting. The crystal was mounted on a glass slide with Dennison's wax, and on top of the crystal a new mask was placed and secured with the same wax. After the cutting methanol was used to dissolve the wax. The Airbrasive cutting gave the most reproducible results.

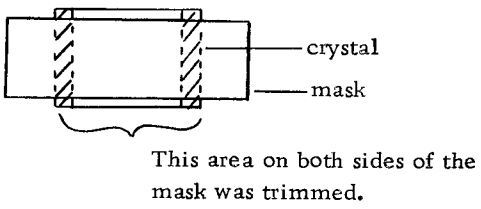


Normally, the crystal was initially prepared for measurements along the $\vec{c}$ axis. After the $\vec{c}$- axis experiment was conducted, gold was evaporated for $\vec{a}$- axis data. Then that part of the crystal which had gold on it for $\vec{c}$- axis readings was removed.

The Airbrasive method was used to cut the Hall coefficient

samples into the desired shape. However, it should be added that the Hall specimens were shaped before gold was evaporated. In addition gold was evaporated on only one side of the Hall samples.

Several other methods of shaping the samples were tried. An ultrasonic cutter literally shattered the crystal into its different layers. A diamond saw was not a satisfactory tool for cutting the sample because often the vibration cracked the crystal.

Soldered contacts were used in all measurements except those on the $\vec{b}$-axis conductivity. After removing all the wax from the crystal, the gold area was cleaned with lactic acid. After the lactic acid had dried, the crystal with a small amount of indium solder and a copper wire "tinned" with indium solder were heated on a hotplate concurrently until the indium solder had melted. The contact was made and then cooled as soon as possible in order to avoid oxidation of the indium. A lead-indium alloy solder also proved satisfactory. No flux was necessary; however the cleaning with lactic acid was crucial. The method outlined above provided contacts that were ohmic, non-rectifying and mechanically stable. Once the contacts were made, the crystal was washed in petroleum ether, acetone, and ethanol in that order. Normally the sample was allowed to soak in ethanol for at least four hours.

# Apparatus and Procedure

## Conductivity

A two-probe system was used in the conductivity measurements. This was found to be the simplest design especially for the low temperature cell to be described. In addition, several other authors (1, 21) have indicated observing identical results with both a two-probe and a four-probe apparatus.

The leads to the crystal were in series with a dc power supply (Keithley Model 240A) and a current-measuring device (Keithley Model 610 Electrometer). For measurements in the $\vec{b}$-axis direction utilizing the guard ring configuration, an additional lead to the crystal was necessary. The circuit for the guard ring configuration was the following:

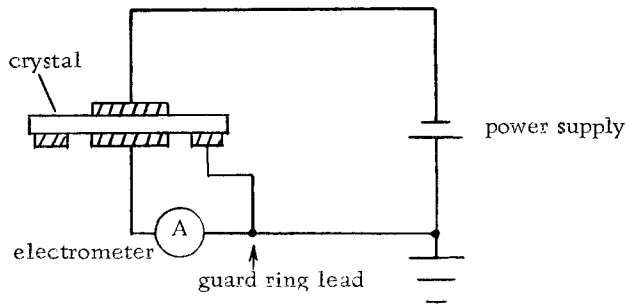


The purpose of this arrangement was to eliminate any contribution due to surface conduction. Unfortunately, due to the geometry of

the crystals, a guard ring could not be used for $\vec{a}$-axis and $\vec{c}$-axis measurements.

A diagram of the low-temperature cell is given in Figure 1. The cell was made of glass, which facilitated easy modification; it was silvered by the Brashear's electroless process to prevent radiation heating. A heavy-gauge aluminum foil was placed around the crystal and thermocouple and secured to the brass block to act as a radiation shield. The leads were all insulated with Teflon. Apiezon W wax was used for the glass-to-metal seal at the capillary input for the leads.

The cell was evacuated constantly and the pressure was .1 microns or less continuously. The pressure was so low, in fact, that it was necessary to place a U-tube trap in liquid nitrogen at the entrance of the cell to prevent the mercury of the McLeod gauge from condensing on the crystal at low temperatures. This was suspected after the gold appeared gray from amalgamation on several crystals.

The sample was cooled by pouring liquid nitrogen into the "cold finger" in the center of the cell after it had been thoroughly evacuated. After reaching the lowest temperature possible, the system was allowed to warm up via heat exchange between the "cold finger" and the air. The cell was immersed in a Dewar flask of liquid nitrogen in order that the outside of the cell might not serve

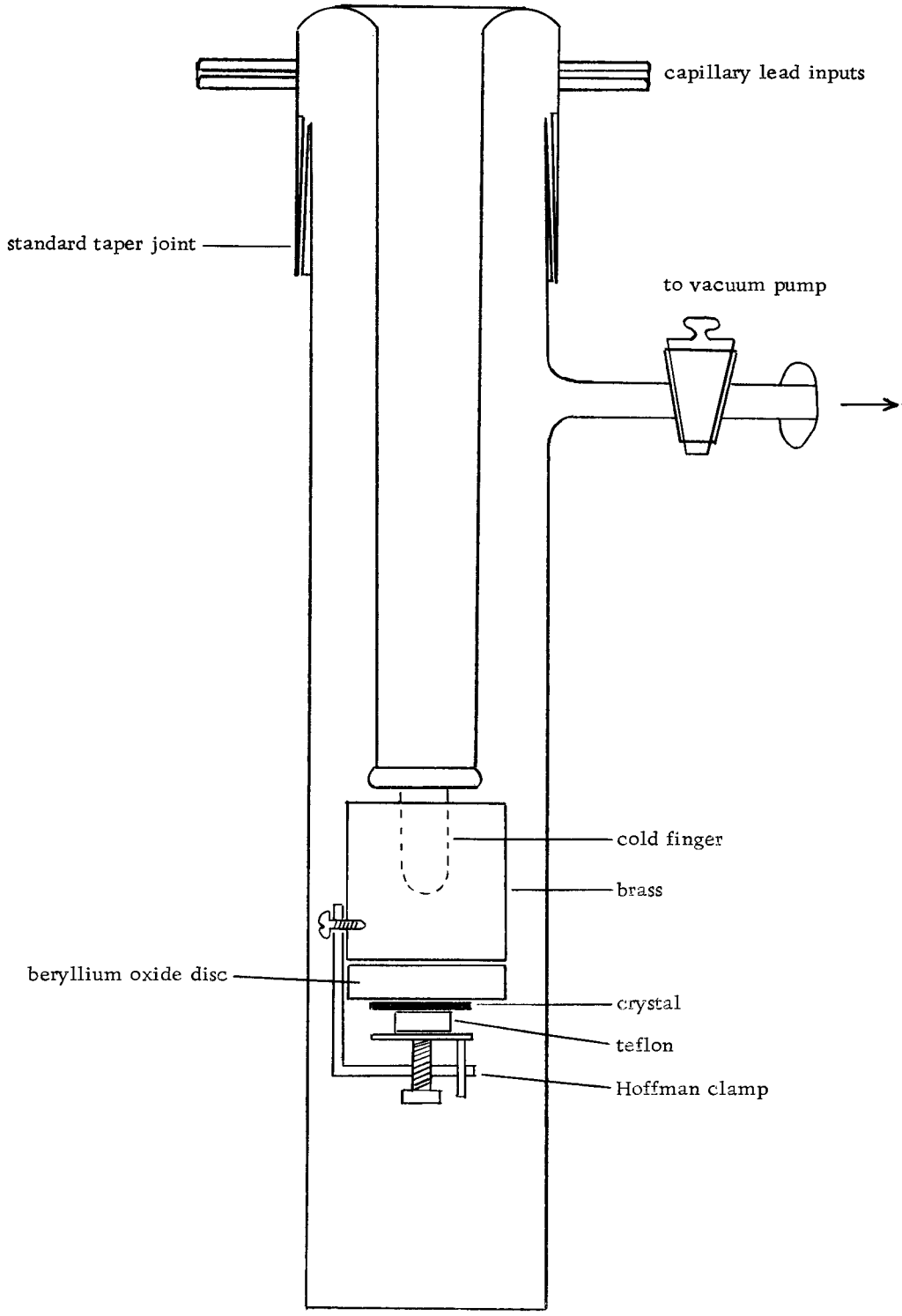


Figure 1. Low temperature electrical conductivity cell

as a radiator at room temperature. This step slowed the warming of the cell significantly. The rate of warming never exceeded $1^{o}C$ every three minutes and was even less at the lower temperatures. The rate at which the system warmed could be controlled by blowing air into the "cold finger." The temperature was monitored by a copper-constantan thermocouple with the bead pressed against the crystal by means of the Teflon block.

For measurements along the $\vec{a}$ and $\vec{c}$ axes, the crystal was placed on a beryllium oxide disc which was clamped against the brass block. A thin layer of Apiezon N grease between the two gave increased heat conduction, and therefore lower temperatures were obtained. Beryllium oxide has a unique set of properties; at room temperature it has a high thermal conductivity, comparable to that of aluminum, while the electrical conductivity is extraordinarily low ($10^{-16}$ $ohm^{-1}cm^{-1}$). Crystal temperatures as low as $-180^{o}C$ were obtained.

For measurements along the $\vec{b}$ axis, the beryllium oxide disc was removed, and the brass block served as one electrode. A copper lead was soldered to the other side of the crystal to complete the circuit. The thermocouple was pressed against the crystal by means of the Teflon block as before. A phosphor bronze spring was used instead of the Hoffman clamp for $\vec{b}$-axis measurements.

## Hall Effect Measurements

dc Apparatus. Since measurements at room temperature only were attempted, the cell used was less elaborate than that used for conductivity data. However, greater efforts were made to shield the system against noise. The crystal was mounted on a glass slide by Dennison's wax. The glass slide was secured on a Lucite block inside an aluminum box used for shielding. Leads from the crystal were soldered to BNC connectors mounted on the grounded aluminum box. Coaxial cables were used throughout the rest of the system and BNC connectors wherever possible. The circuit diagram is given in Figure 2. The dc power supply was a Keithley Model 241 and the microvolt-ammeter was a Keithley Model 150A. The rheostat used was a 10-turn helipot. Currents of up to 0.2 mA passed through the crystal; greater currents heated the sample, thus changing its resistance. After establishing the current by setting the applied voltage across the crystal, the helipot was adjusted to read a null voltage on the microvoltmeter. The magnetic field was then applied and the Hall voltage observed on the microvoltmeter. The magnetic field was supplied by a Varian 6" Electromagnet Model V-4007 in conjunction with a Varian regulated magnet power supply Model V-2200A.

Measurements on a sample of n-type silicon were made to

test the system. The signal observed on the microvoltmeter was proportional to the magnetic field and to the current passing through the specimen indicating that the appratus was functioning properly.

ac Apparatus. An ac system was assembled and lower voltages could be observed. The circuit is given in Figure 3. This system utilizes a Princeton Applied Research Lock-In Amplifier Model JB5, a highly selective frequency phase detector. In conjunction with the lock-in amplifier, a Tektronix Type 122 low level preamplifier with a gain of 1000 was used. The current source was an Exact Electronics frequency generator. A ten kilo-ohm rheostat was connected at the output in order to adjust the current through the sample. An audio transformer was placed in the circuit to alleviate a grounding problem. For the ac system, shielding the leads inside the aluminum box prevented capacitive coupling and reduced the noise levels. A full scale range of ten microvolts could be achieved without noticeable noise hindrance.

The procedure for measuring the Hall effect with the ac system was similar to that of the dc apparatus. A current of 0.2 mA was passed through the crystal. With the ac system it was necessary to tune the detector to the frequency and phase of the current in the crystal; this was achieved by maximizing a small voltage observed on the voltmeter due to a helipot setting adjusted to give a little

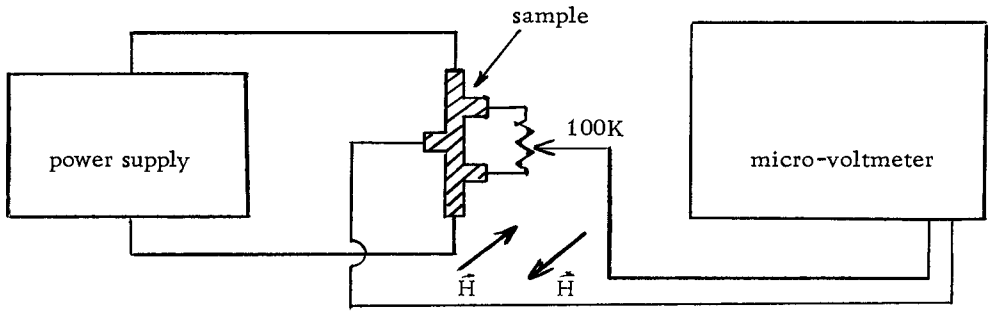


Figure 2. dc Hall effect measurement apparatus

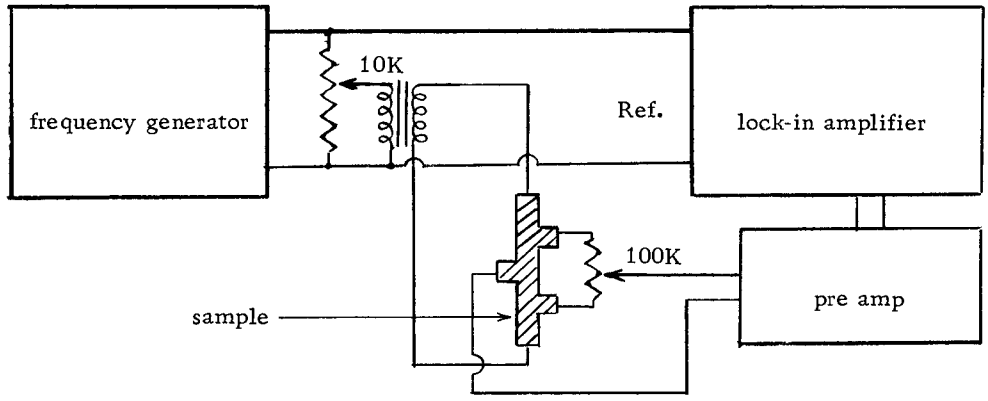


Figure 3. ac apparatus

signal. The 100 kilo-ohm helipot was adjusted until the voltmeter on the lock-in amplifier indicated a null signal. This step had to be repeated each time a more sensitive scale was selected. If the current through the crystal were changed, the helipot had to be adjusted again. The dc magnetic field of six kilogauss was then applied. The Hall voltage was observed on the voltmeter of the lock-in amplifier.

# RESULTS

## Conductivity Measurements

The conductivity of the crystals was measured with the electric field parallel to each of the three crystallographic directions. Measurements at temperatures as low as -165°C were achieved in all cases, and often lower values were obtained. Conductivity curves in the $\vec{a}$, $\vec{b}$ and $\vec{c}$ directions are given in Figures 4, 5 and 6 respectively. Data for several crystals are given for each axis. This serves to indicate the degree of reproducibility of the data. While discrepancies are found, one should add that Boros noted that crystals of different origin had conductivities which differed by as much as an order of magnitude (5).

Over the temperature range -75°C to 25°C, the conductivity ($\sigma$) is described by the Arrhenius equation

$$\sigma = \sigma_0 e^{-E/2kT}$$

where E is the activation energy of conduction and $\sigma_0$ is a constant. An explanation for the factor of 1/2 in the exponent is given later (see page 42). The activation energy can be found from the slope of curves in which $\log \sigma$ is plotted with respect to reciprocal temperature. The activation energies were calculated from the linear

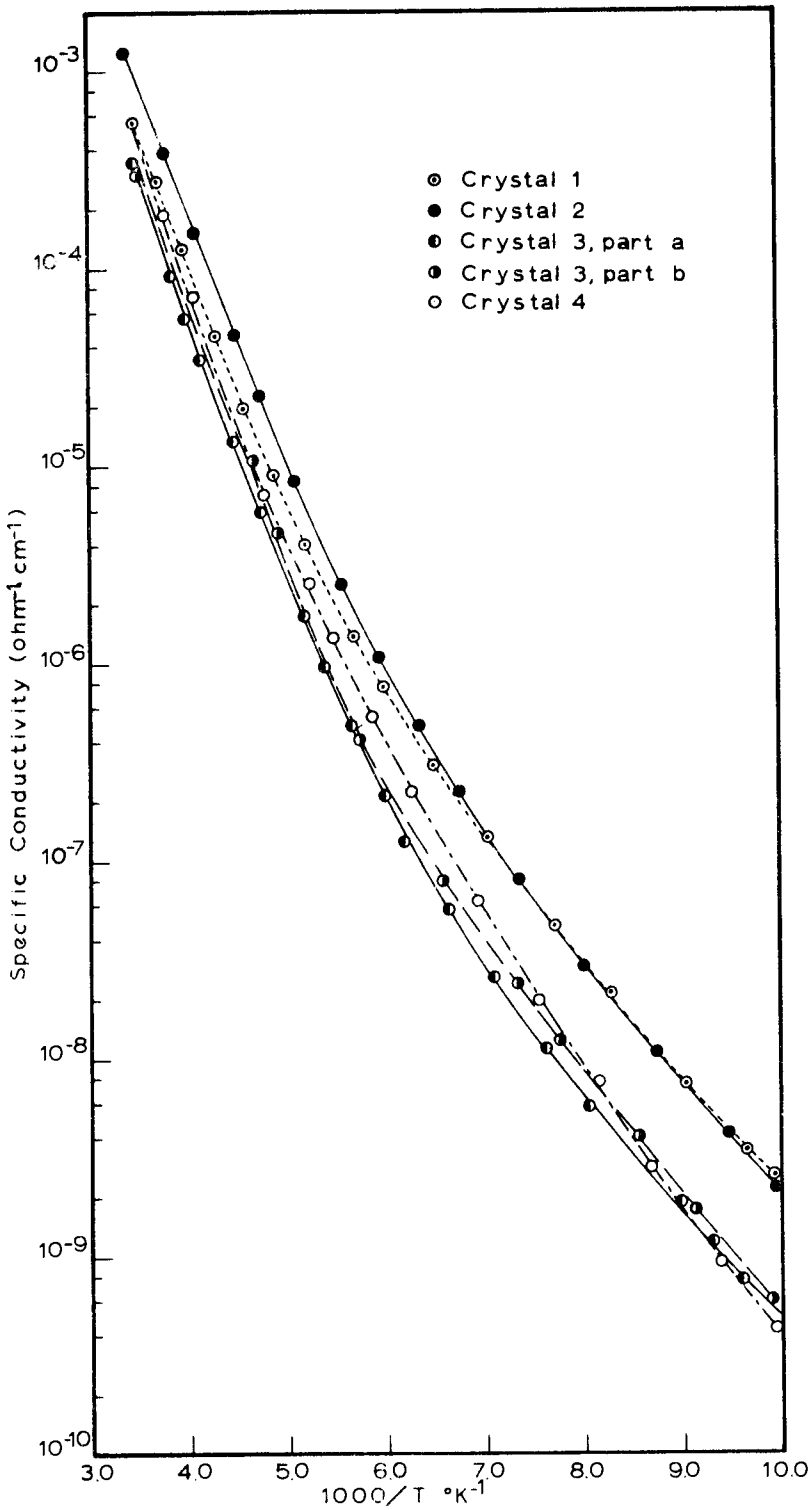


Figure 4. Conductivity of $V_2O_5$ in the a-axis direction

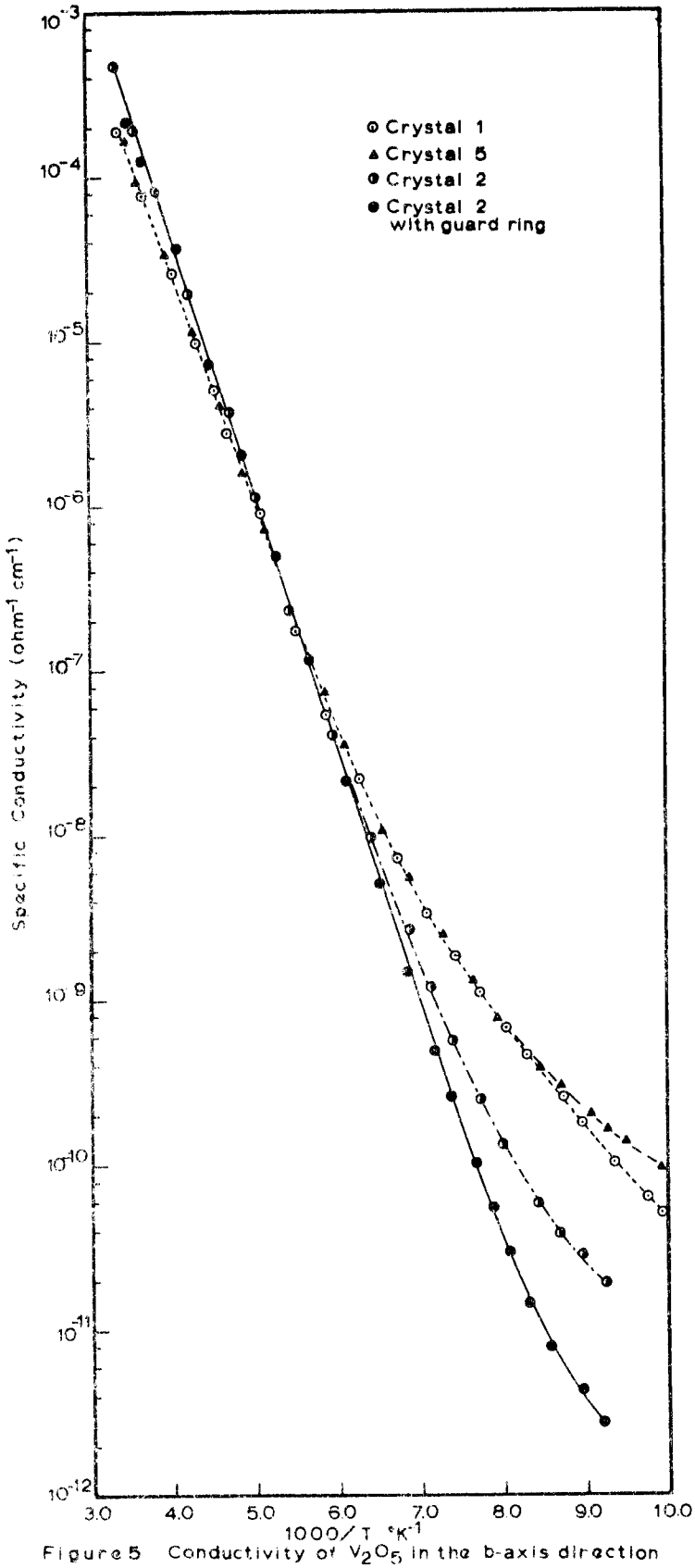


Figure 5 Conductivity of $V_2O_5$ in the b-axis direction

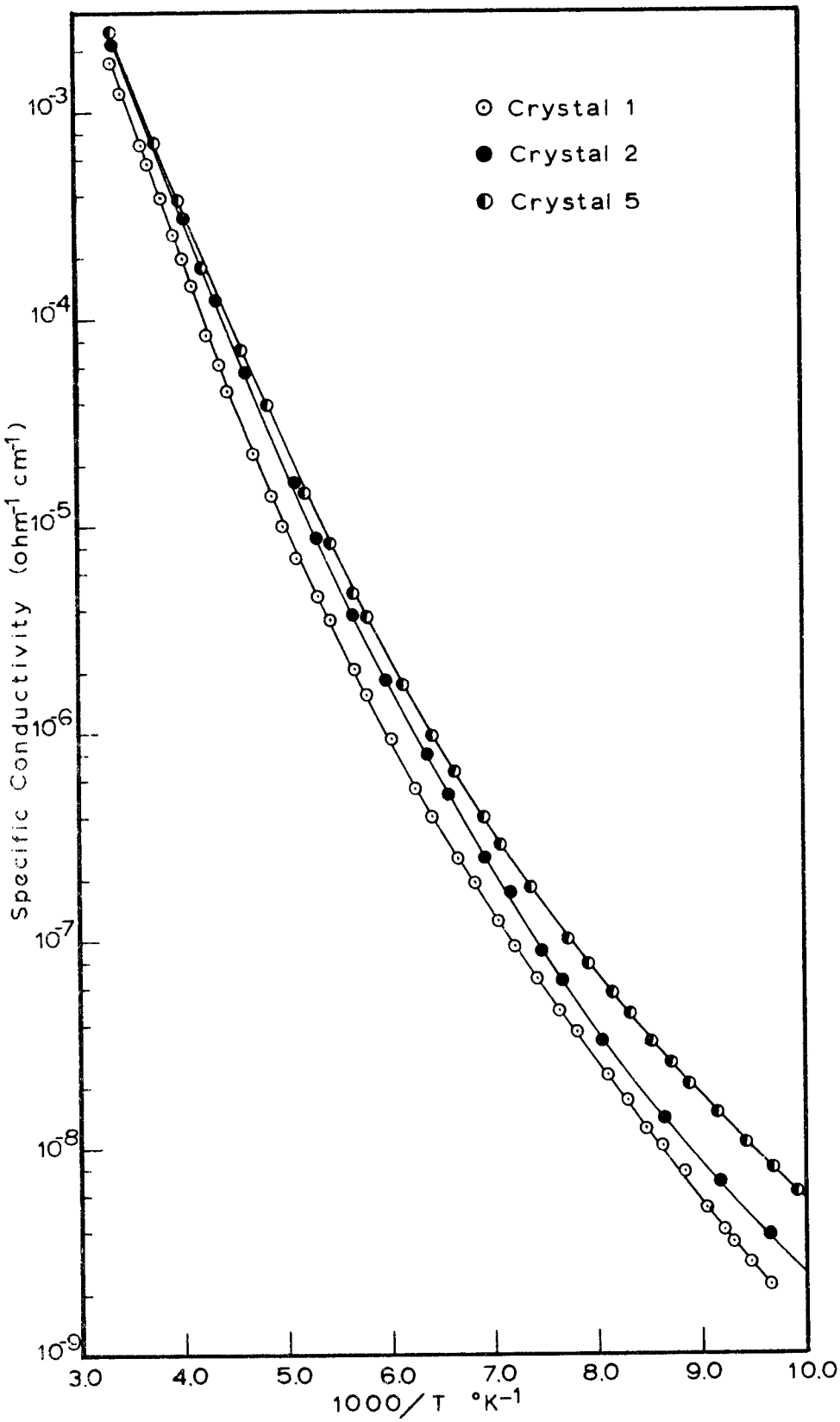


Figure 6. Conductivity of $V_2O_5$ in c-axis direction

portion of the curves near room temperature and are given in Table 1.

Table 1

| Axis | Average V-V Distance[1] (angstroms) | Maximum V-V Distance[3] (angstroms) | Activation Energy (electron volts) | Conductivity at 0°C ($ohm^{-1} cm^{-1}$) |
|---|---|---|---|---|
| a | 3.27 | 3.42 | $.56 \pm .02$ | $2.3 \times 10^{-4}$ |
| b | 4.37 | 4.37 | $.58 \pm .02$ | $1.2 \times 10^{-4}$ |
| c | 3.56 | 3.08 | $.54 \pm .02$ | $6 \times 10^{-4}$ |

Figure 7 gives a comparison of the conductivity behavior in the three crystallographic directions. The plots were compiled by taking the minimum conductivity curves from each of the three preceding figures. The minimum curves are compared because it was assumed that they were the most nearly correct. This assumption was made because it is more likely to have positive contributions to the conductivity than negative contributions.

Such positive contributions include surface conduction, impurity effects, and extraneous leakage paths. Measurements of the resistance of the cell without a sample were made at low temperatures to determine if any leakage paths in the cell were present. The resistance was found to be at least three orders of magnitude greater than that of the sample at a comparable temperature. Precautions

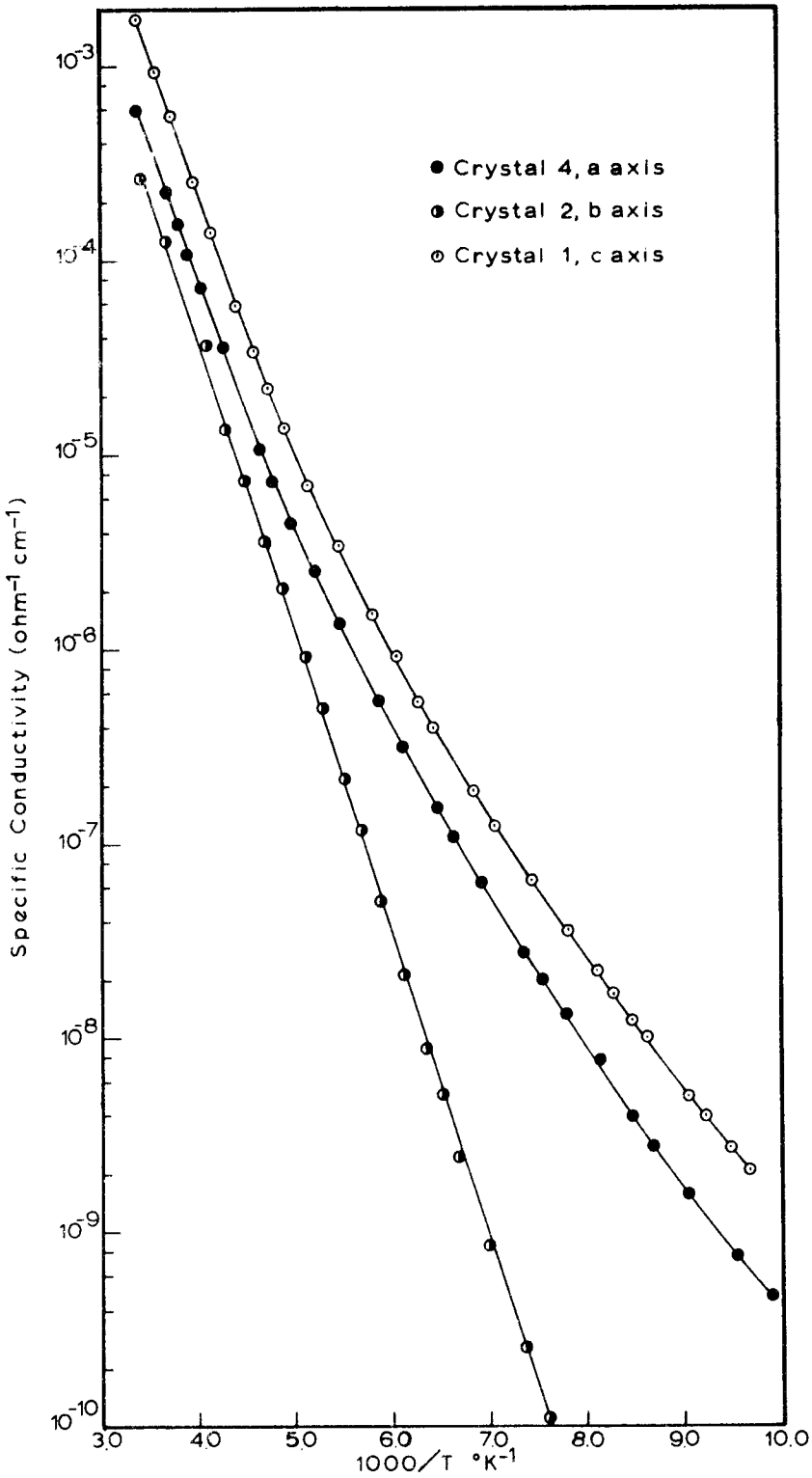


Figure 7. Comparison of conductivity along the various axes

to guard against impurities were described in the experimental section.

A guard ring to eliminate surface conduction was used to obtain one of the $\vec{b}$-axis curves. The thin crystals did not allow this configuration on measurements along the $\vec{a}$ and $\vec{c}$ axes. The data obtained varied from that taken without a guard ring. The interpretation of this result will be discussed later.

Hall Effect Measurements

dc Apparatus. Exhaustive attempts were made to minimize the noise of this system. However a level of 50 microvolts could not be eliminated. No Hall effect signal was detectable on $V_2O_5$.

ac Apparatus. With the ac apparatus, lower voltages could be measured. However when higher-sensitivity scales were utilized, the joule heating of the crystal became more apparent. Thus, as more sensitive scales were achieved, the current had to be reduced nullifying some of the increased sensitivity. At very high sensitivity the power supply of the magnet began to perturb the readings.

Nevertheless, an upper limit on the Hall voltage could be established. From the measurements that were made, one could conclude that the Hall voltage was not greater than 20 microvolts when .14 mA was passed through the crystal placed in a magnetic

field of 5000 gauss. The crystal thickness was .025 cm. The Hall coefficient is given by the relation (22, p. 99)

$$R_H = \frac{V_H d}{IB\,10^{-8}}$$

$$R_H = 71\ \text{cm}^3\,\text{coul}^{-1}$$

The conductivity of the sample described above was $5.46 \times 10^{-3}\ \text{ohm}^{-1}\ \text{cm}^{-1}$. The Hall mobility is defined as

$$\mu_H = R_H \sigma$$

$$\mu_H = 0.4\ \frac{\text{cm}^2}{\text{volt sec.}}$$

From the Hall coefficient the number of carriers can also be calculated providing the classical model of free electron conduction is assumed. While this model may not be correct for $V_2O_5$ conduction, it may be of interest to calculate the number of carriers.

$$n = \frac{3\pi}{8}\ \frac{1}{R_H e}$$

$$n = 1 \times 10^{17}\ \text{cm}^{-3}$$

The calculated Hall coefficient and mobility are upper limits; the number of carriers calculated is a lower limit.

# DISCUSSION

The conductivity data presented provide a set of curves which differ less than an order of magnitude at any given temperature and the curves are of similar shape, with slight differences which may be due to anisotropy. The curves are linear from room temperature down to at least -75°C. At lower temperatures a small curvature is observed. The degree of curvature is so consistent that one is tempted to devise a model to explain it.

However, the data taken with the guard ring configuration deviates from that taken without it. This is strong evidence that surface conductivity becomes significant at low temperatures. The linear plot complies with the Arrhenius relation down to -160°C. If surface conduction is the phenomenon being measured from -120°C to -160°C without the guard ring in the $\vec{b}$-axis direction, then it is reasonable to generalize this result to measurements along other axes. This would imply that the curvature at low temperature is due to surface conduction.

In light of this information, one becomes suspicious of previous conductivity measurements taken in the low temperature region by other authors. This might explain the wide variation of conductivity data which is present in the literature. Figure 8 is a sampling of several other authors' results for $V_2O_5$.

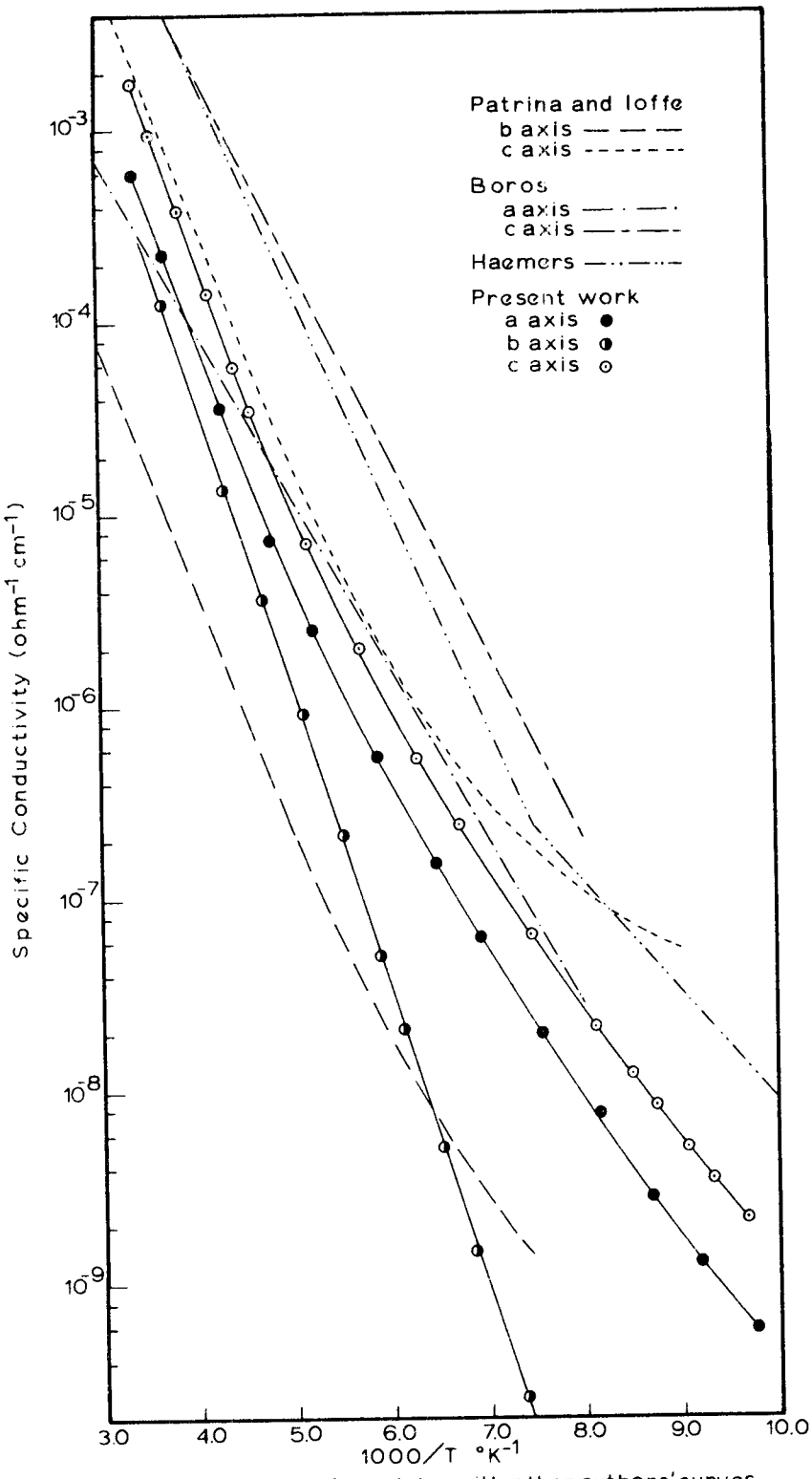


Figure 8. Comparison of the data with other authors' curves

Patrina and Ioffe interpret their data as curves with a lower activation energy at lower temperatures (21). The agreement with the $\vec{c}$-axis conductivity is good down to -130°C where their plots begin to exhibit much more curvature than the present work. Likewise their $\vec{b}$-axis plot begins to exhibit a lower activation energy at -110°C. They support their observed change in activation energy with electron paramagnetic resonance (EPR) studies (14). At higher temperatures they claim that $V^{4+}$ becomes $V^{5+} + e^{-}$, and consequently a higher activation energy is necessary for conduction. In the present work the results found on $\vec{b}$-axis measurements with a guard ring show no change in activation energy down to -160°C. This indicates that Patrina and Ioffe may have been measuring surface conduction, and therefore no model of bulk conduction is necessary to explain any change in slope.

The conductivity plots of Haemers display two straight lines of different slopes intersecting at about -130°C (12). In his paper Haemers states that the temperature at which the "knee" occurred was dependent on the degree of purity of the crystal. This result suggests impurity conduction in the low temperature region. Boros made measurements down to -150°C in the $\vec{a}$ and $\vec{c}$ directions (5). He interpreted his data as complying with the Arrhenius relation.

After reviewing the data of several authors and noting the variety of interpretations, one must observe that any conclusion is

questionable. Nevertheless, it appears as though most of the curves in the present work exhibit surface conductivity below -120°C with the exception of the $\vec{b}$-axis measurements with a guard ring. The linearity of this curve indicates that an Arrhenius-type equation is applicable for conductivity in the $\vec{b}$-axis direction down to -160°C. At lower temperatures some deviation from linearity is observed; and since surface conductivity has been eliminated, this is probably due to impurities similar to the phenomenon exhibited in Haemers' results.

The most commonly accepted mechanism for describing semiconducting behavior in mixed valence, transition-metal oxides is the polaron or "hopping" mechanism. Evidence that lower valence states of vanadium are present is strong, not only because of the dissociation of $V_2O_5$ during crystal growth as shown by Milan (18), but also EPR results on pure specimens show vanadium in the +4 state (10, 14).

The polaron theory purports that ions of a valence different from that of the host crystal ions tend to distort or polarize the neighboring ions. For conduction to occur an electron must be transferred to a neighboring cation, and consequently the site of polarization moves through the lattice. Therefore the observed value of the activation energy is normally not one of carrier production but rather of mobility.

Most of the data on controlled-valence semiconductors has been done on lithium-substituted nickel oxide. The model that $Li^{1+}$ substitution into the lattice yielded $Ni^{3+}$ in addition to the host $Ni^{2+}$ was originally proposed by Verwey (23). Arguments used to support the polaron theory in NiO are the following: (6, 13)

a) The conductivity at room temperature is proportional to the lithium concentration.

b) A low Hall effect, and therefore a low mobility, are observed.

c) In most semiconductors when the impurity concentration is above $10^{-6}$ mole %, the semiconductor becomes degenerate. As degeneracy develops the activation energy decreases to a very low level until metallic conduction is realized. However, the activation energy at high lithium concentrations (>5 mole %) is still rather large. At such concentrations, however, nearly all nickel ions have lithium neighbors, so that the $Ni^{3+}$ holes can move through the lattice without leaving the $Li^{1+}$ ions. The temperature dependance of the conductivity then must be due to a migrational activation energy.

In $V_2O_5$ the lattice would be polarized in the neighborhood of each $V^{4+}$ resulting in a polaron. Evidence to support the polaron conduction mechanism in $V_2O_5$ is the following:

a) Ioffe and Patrina found that the room temperature conductivity of $V_2O_5$ is proportional to the $V^{4+}$ concentration (14).

b) The mobility as determined from the Hall measurements in the present work was found to be low.

c) The impurity concentration in $V_2O_5$ is relatively high (e.g., 1-2% $V^{4+}$, $10^{-3}$% Fe, $10^{-2}$% Pt). However, semiconduction still prevailed. Figure 8 shows a wide variation in conductivity values at a given temperature yet the activation energies change only slightly. In another paper Patrina and Ioffe doped $V_2O_5$ crystals with .1% molybdenum and the same temperature dependence and conductivity as in their pure samples was found (9).

From the parallel arguments outlined above, one can say that the polaron theory serves to explain much of the conductivity behavior in $V_2O_5$. Further evidence in support of polaron theory is that the conductivity at a given temperature increases as the maximum vanadium to vanadium (V-V) distance decreases as observed in Table 1. For example, the conductivity is highest in the $\vec{c}$-axis direction where the V-V distance is shortest; likewise the conductivity is lowest in the $\vec{b}$-axis direction where the V-V distance is greatest. The closer the cations, the greater the overlap of the wave functions. This gives a larger electron tunneling probability and consequently a higher conductivity.

Allersma, et al. (1) have argued that the conductivity should decrease as the average V-V distance increases. They determined their average value for the $\vec{a}$ axis by summing the distance between 1 to 2 and 2 to 4 and dividing by two (see Figure 9). They considered the average distance in the $\vec{c}$ direction to be the distance from 1 to 3. In the present work the maximum distance in the $\vec{c}$-axis direction was taken to be the distance between 1 and 2 since it was assumed the polaron moved by this route. However, one could propose that the average V-V distance is of little significance, but rather the maximum V-V distance is the quantity of interest since it is rate-determining in the conduction process.

The $V_2O_5$ crystal structure can be seen in Figure 9. It is likely that conduction in the $\vec{c}$-axis direction occurs by an electron "hopping" from cations $1 \rightarrow 2 \rightarrow 3$ rather than hopping from $1 \rightarrow 3$. This seems logical not only because it is a shorter distance from 1 to 2 and 2 to 3 (3.08 A) compared to 1 to 3 (3.56 A) but also because the electron does not have to surmount the potential barrier of the oxide ion in its path. For conduction to occur in the $\vec{a}$-axis direction, the electron must "hop" from cation 2 to 4. A similar situation occurs for conduction in the $\vec{b}$-axis direction. It can be seen that for a polaron to move in the $\vec{a}$ and $\vec{b}$-axis directions an electron must tunnel through an oxygen ion. However, for a polaron to move in the $\vec{c}$-axis direction, no oxygen ion obstructs its path.

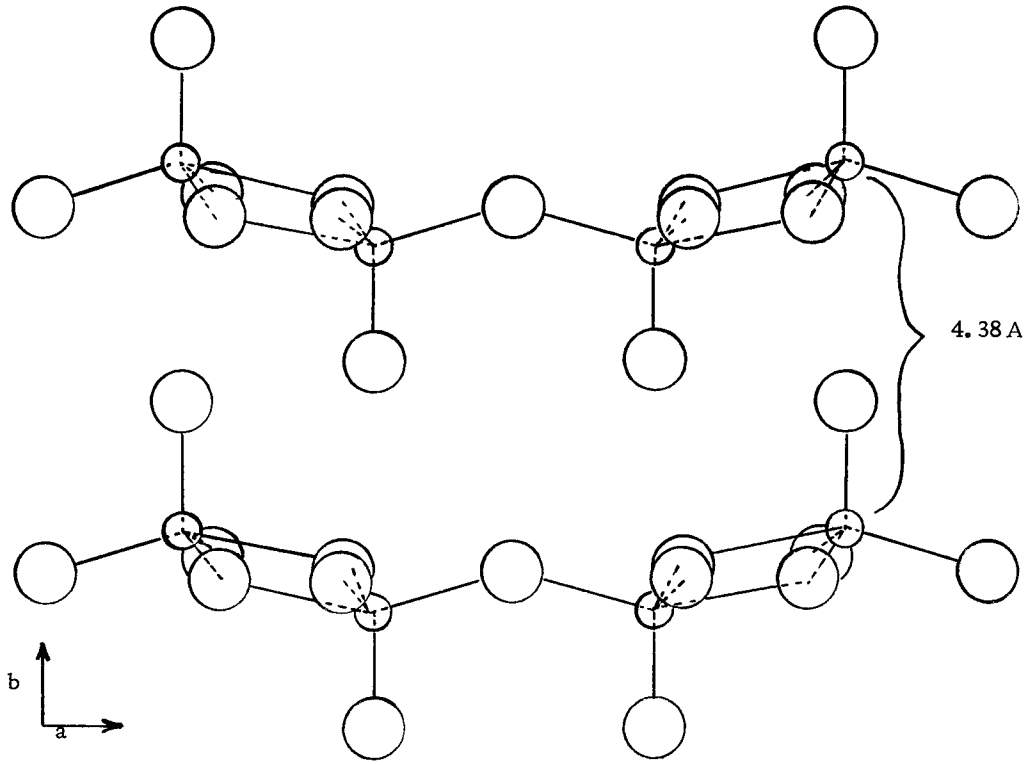


Figure 9a. Projection of $V_2O_5$ structure onto the 001 plane (7).

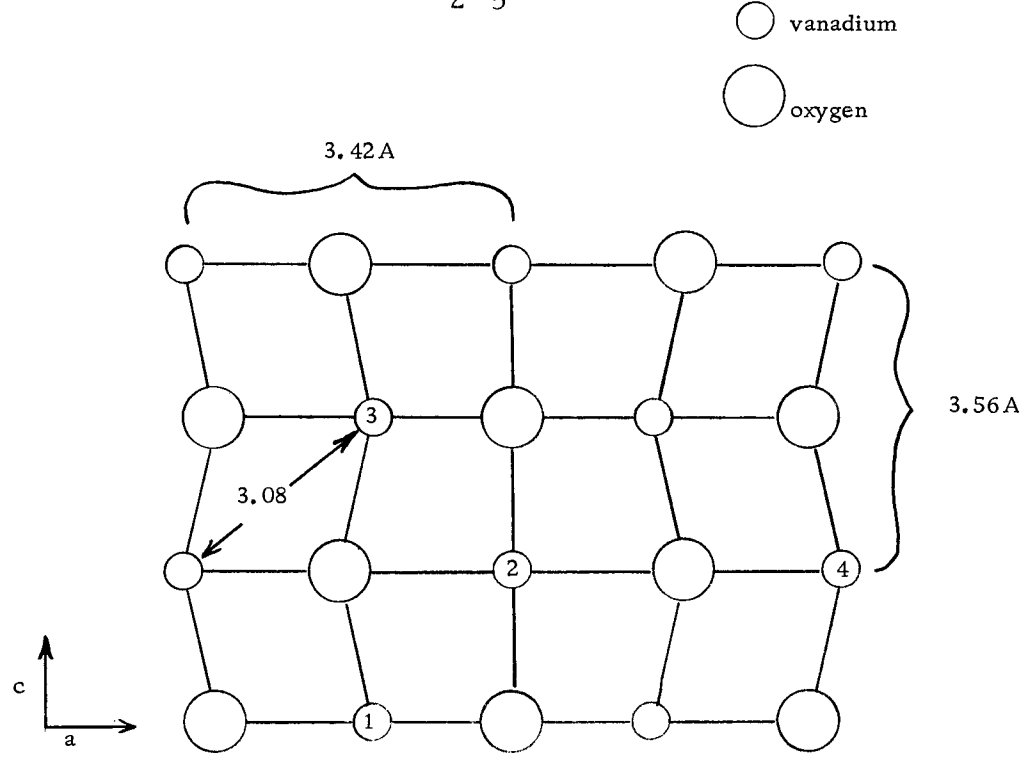


Figure 9b. Projection of $V_2O_5$ structure onto the 010 plane

Considering the anisotropy of the crystal structure and of the conduction process, one would expect to observe different activation energies for conductivities measured in the three directions. However these do not differ significantly considering the experimental error (see Table 1).

The activation energy may be made up of a carrier production term and a transport term. Of these the transport term is expected to be anisotropic. However Mott indicates that below one-half the Debye temperature, ($\theta_D$), the mobility of a polaron is constant; whereas above that temperature the mobility should vary exponentially with temperature (20). The Debye temperature of $V_2O_5$ is unknown. The Debye temperature of MgO is 946°K, $TiO_2$ 758°K, $Fe_2O_3$ 660°K (11, p.4-62). By comparison with other oxides, it is believed that the temperature region examined was below $\frac{\theta_D}{2}$. Therefore the transport term should be a constant throughout the entire range but have a different value for conduction in different directions. Thus, we must consider the carrier production term to find the temperature dependence of the conductivity. The carrier production term would be isotropic; and since small anisotropic effects are observed, one could conclude that it is a much larger contribution to the activation energy than the transport term.

Gillis and Boesman have studied $V_2O_5$ crystals with EPR (10). They found $V^{4+}$ present and made a study of the changes in the

spectrum on different crystal orientations. They concluded that associated with each $V^{4+}$ site is an oxygen vacancy. The energy required to remove an electron from the $V^{4+}$ -vacancy center can be considered to be the carrier production or ionization energy. To calculate this energy a knowledge of the dielectric constant is necessary but it is unavailable. However, let us assume that the ionization energy constitutes all of the activation energy, for it was argued above that the transport term is much smaller. Utilizing an electrostatic calculation, one can calculate an approximate dielectric constant of $V_2O_5$ assuming the activation energy is that energy necessary to free the electron from the $V^{4+}$ -vacancy center. If the oxygen vacancy is considered to have a charge of +2 and the diameter of the center is $2 \times 10^{-10}$ m - since this is the distance between the nucleus of $V^{4+}$ and the vacancy - then we obtain the following result:

$$E_{act.} = \frac{1}{4\pi\epsilon_0} \frac{q_1 q_2}{K R}$$

$$K = 25$$

In the above calculation the activation energy used was .56 ev but converted to $9 \times 10^{-20}$ joules; $\epsilon_0$ is the permittivity of free space, $8.85 \times 10^{-12}$ coul$^2$/nt-m$^2$.

Dielectric constants for other oxides are the following: (18, p. 452-494) $Ta_2O_5$ 11.6, $Cr_2O_3$ 12.0, PbO 26, $TiO_2$ 48, and $VO_2$ 26 (19).

Considering the values for other oxides, one finds the calculated value above to be a reasonable result.

In summary, the electron in the $V^{4+}$-vacancy center is thermally ionized and moves from site to site with the corresponding lattice distortion (polaron). The measurements made in the present work were below $\frac{\theta_D}{2}$ ; therefore the mobility of the polaron is constant. The main contribution to the activation energy is that energy required to remove an electron from the $V^{4+}$-vacancy center. This model not only gives an explanation of the lack of anisotropy in the activation energies observed but also yields a reasonable value for the dielectric constant of the crystal. The reaction may be written as follows:

$$V^{4+}[O^{=}] \rightleftharpoons e^{-} + V^{5+}[O^{=}]$$

Let $n$ = the concentration of "free electrons," $e^{-}$

$n_c$ = the concentration of the $V^{4+}$-vacancy complex, $V^{4+}[O^{=}]$

$n_c^{+}$ = the concentration of the ionized complex, $V^{5+}[O^{=}]$

Then we can define an equilibrium constant, K, as

$$K = \frac{n\, n_c^{+}}{n_c} = e^{-\Delta\tilde{G}/kT}$$

where $\Delta\tilde{G}$ is the reaction potential for the above process.

Since $n = n_c^+$, we can write

$$n^2 = C\, e^{-E/kT}$$

$$n = C^{1/2}\, e^{-E/2kT}$$

where $C = n_c e^{\Delta S/k} = n_c \left(\frac{2\pi mkT}{h^2}\right)^{3/2}$.

Here the approximation is made that $E$ is equal to the enthalpy change for the process considered. Since $\sigma = ne\mu$ with $e$ a universal constant and $\mu$ (the mobility) a constant in the temperature region considered, then the conductivity ($\sigma$) is dependent on the thermal generation of carriers (n). The activation energies were calculated assuming $\sigma = \sigma_O e^{-(E/2kT)}$ since $n \sim e^{-E/2kT}$.

At higher temperatures above $\frac{\theta_D}{2}$, the observed activation energy would change because the transport term becomes a factor in the activation energy. The observed activation energy is found from the slope of the log $\sigma$ curve with respect to reciprocal temperature. The ionization energy does not change; however, the predicted mobility varies as $e^{-W/kT}$ at higher temperatures (above $\frac{\theta_D}{2}$). W is defined as the activation energy of the mobility. Therefore, the observed activation energy should increase and become E + W at high temperatures. However, the data of Patrina and Ioffe, and Haemers indicate that the activation energy decreases at high temperatures. This may be due to either the mobility factor lowering

the observed activation energy, the exhaustion of carrier supply at high temperatures, or some impurity effect. From calculations considering the exhaustion of carriers, the effect is negligible at $500^{o}K$, the temperature where the curves deviate from linearity. Even at $1000^{o}K$ the deviation is only 4%. Therefore, either the mobility at higher temperatures does not behave as the model predicts or else impurities produced anomolous results.

Although the activation energy of conduction is isotropic, the observed conductivity is anisotropic. This can be explained by examining the two steps in the conduction mechanism more closely. The first step is considered to be the ionization of the electron from the $V^{4+}$-vacancy center. This step is isotropic, but it determines the rate of the conduction process because of the strong electrostatic attraction of the $V^{4+}$-vacancy center relative to the normal $V^{5+}$ site.

The second step in the conduction mechanism is the electron moving from one normal $V^{5+}$ site to a neighboring $V^{5+}$ site. This part of the process is anisotropic because it is dependent on the distance between the cations. More specifically, the mobility is anisotropic due to the different potential field which the electron encounters in traveling through the anisotropic crystal. The anisotropy of the mobility accounts for the variation in the conductivity

in the three crystallographic directions. However, the relative values of the mobility must be constant because the conductivity curves are parallel.

In the model of the $V^{4+}$ oxygen-vacancy center proposed by Gillis and Boesman (10), it is indicated that for every two $V^{4+}$-oxygen-vacancy centers present one $V^{3+}$ cation must be present in order to maintain charge balance in the crystal. Therefore, it should be added that a $V^{3+}$ site is a possible source of conduction electrons in addition to the $V^{4+}$-vacancy center. However, this addition does not change the conclusions of the model. The ionization of the $V^{3+}$ site would yield isotropic values for the activation energy. However, the conductivity is anisotropic because the ensuing polaron movement is anisotropic due to the different V-V distances in the three crystallographic directions.

# SUGGESTIONS FOR FURTHER WORK

1. Although attempts to measure the Hall effect were unsuccessful, the author feels that the measurements could be made in view of advancing technology. A low noise field effect transistor pre-amplifier when used in conjunction with an ac electric and magnetic field would probably produce a high enough signal-to-noise ratio to make it possible to observe a signal. This experiment would be the most useful in studying the conduction mechanism further. In addition, Seebeck effect measurements would be useful for the same purpose.

2. A study of the conductivity with different amounts of impurities, preferably vanadium in the +4 state would be enlightening. Possibly growing the crystals under various oxygen pressures would yield different amounts of defects. However, if this were unsuccessful, doping with molybdenum or copper would reduce the vanadium to a known concentration of vanadium in the +4 state.

3. It would be of interest to determine the static dielectric constant from ac conductivity measurements. This could be compared with the calculated value in the present work.

4. As indicated earlier surface conductivity will prevail at low temperatures unless a guard ring is used. In order to have a guard ring configuration for measurements in the $\vec{a}$ and $\vec{c}$-axis directions, thicker crystals must be grown. It has been reported

that $V_2O_5$ single crystals were grown by the Kyropoulos method (10). Perhaps this would yield crystals suitable for a guard ring configuration so that reliable conductivity measurements at low temperatures could be made.

# BIBLIOGRAPHY


1. Allersma, T., R. Hakim, T. N. Kennedy and J. D. Mackenzie. Structure and physical properties of vanadium pentoxide. Journal of Chemical Physics 46:154-160. 1967.

2. Andersson, G. Studies on vanadium oxides. Acta Chemica Scandinavica 8:1599-1606. 1954.

3. Bachmann, H. G., F. R. Ahmed and W. H. Barnes. The crystal structure of vanadium pentoxide. Zeitschrift für Kristallographie 115:110-131. 1961.

4. Barker, A. S., Jr., H. J. Guggenheim and H. W. Verkur. Infrared optical properties of vanadium dioxide above and below the transition temperature. Physical Review Letters 17:1286-1289. 1966.

5. Boros, J. Elektrische und optische Eigenschaften von vanadiumpentoxyd Kristallen. Zeitschrift für Physik 126:721-724. 1949.

6. Bosman, A. J. and C. Crevecoeur. Mechanism of electrical conduction in Li-doped NiO. Physical Review 144:763-770. 1966.

7. Byström, A., O. Brotzen and K. A. Wilhelmi. Vanadium pentoxide - a compound with five coordinated vanadium atom. Acta Chemica Scandinavica 4:1119-1130. 1950.

8. Chamot, E. M. Elementary chemical microscopy. 2d ed. New York, John Wiley, 1921. 479 p.

9. Dmitrieva, L. V., V. A. Ioffe and I. B. Patrina. The relationship between electrical conductivity and the state of the $V^{4+}$ ions in $V_2O_5$ crystals. Soviet Physics - Solid State 7:2228-2231. 1966. (translated from Fizika Tverdogo Tela)

10. Gillis, E. and E. Boesman. E. P. R. studies of $V_2O_5$ single crystals. Physica Status Solidi 14:337-347. 1966.

11. Gray, D. E. (coordinating ed.), American Institute of Physics Handbook. 2d ed. New York, McGraw-Hill, 1963. 2112 p.

12. Haemers, Johan. Sur la conductivité electrique du $V_2O_5$. Comptes Rendus de l'Academie des Sciences, Paris 259:3740-3743. 1964.

13. Heikes, R. R. and W. D. Johnston. Mechanism of conduction in Li-substituted transition metal oxides. Journal of Chemical Physics 26:582-587. 1957.

14. Ioffe, V. A. and I. B. Patrina. Electron paramagnetic resonance in single crystals of vanadium pentoxide. Soviet Physics - Solid State 6:2425-2428. 1965. (translated from Fizika Tverdogo Tela)

15. Kachi, S., K. Kosuge and T. Takada. Electrical conductivity of vanadium oxides. Journal of the Physical Society of Japan 18:1839-1840. 1963.

16. King, B. W. and L. L. Suber. Some properties of the oxides of vanadium and their compounds. American Ceramic Society Journal 38:307-311. 1955.

17. Landolt, Hans Heinrich and Richard Börnstein. Zahlenwerte und Funktionen aus Physik, Chemie, Astronomie, Geophysik und Technik. Band II. Eigenschaften der Materie in ihren Aggregatzuständen. Teil 6. Elektrische Eigenschaften I. 6. Auflage. Berlin, Springer-Verlag, 1959. 1018 p.

18. Milan, E. F. The dissociation pressure of vanadium pentoxide. Journal of Physical Chemistry 38:498-508. 1929.

19. Morin, F. J. Oxides of the 3d transition metals. Bell System Technical Journal 37:1047-1083. 1958.

20. Mott, N. F. Electrons in disordered structures. Advances in Physics 16:49-144. 1967.

21. Patrina, I. B. and V. A. Ioffe. Electrical properties of vanadium pentoxide. Soviet Physics - Solid State 6:2581-2585. 1965. (translated from Fizika Tverdogo Tela)

22. Putley, E. H. The hall effect and related phenomena. London, Butterworths, 1960. 263 p.

23. Verwey, E. J. W., P. W. Haaijman, F. C. Romeyn and G. W. van Oosterhout. Controlled-valency semiconductors. Phillips Research Reports 5:173-187. 1950.